

# Mechanisms governing the ‘gasification to char oxidation transition’ in counter-current flame propagation in packed beds: insights from single-particle experiments

Mani Kalyani Ambatipudi <sup>\*1</sup>, Jaganathan V M<sup>1</sup>, and Varunkumar S<sup>1</sup>

<sup>1</sup>*Department of Mechanical Engineering, IIT Madras, Chennai, India*

October 16, 2021

## Abstract

Mechanisms governing the *gasification to combustion regime transition* in counter-current packed bed biomass systems are investigated in the current work. Single-particle experiments are performed with different oxidizer streams (air, mixtures of O<sub>2</sub>/CO<sub>2</sub>) to bring out the role of *the extinction of the envelope non-premixed ‘volatiles’ flame and simultaneous volatile-char combustion at the stagnation point* on the transition to char oxidation in packed beds. Results indicate that for O<sub>2</sub> fractions lower than 23% (w/w), the transition is governed by the extinction of the envelope diffusion flame. At higher O<sub>2</sub> fractions, typically > 32% (w/w), simultaneous volatile-char oxidation at the stagnation point drives the transition to char combustion. The strain rates computed at ‘gasification to char combustion transition’ from earlier studies with air and O<sub>2</sub> fractions  $\leq 23\%$  (w/w) in the oxidizer streams coincide with the strain rates obtained at the transition from classical envelope flame to a wake flame with single particles. Velocities

---

\*manikalyani24@gmail.com

at which simultaneous oxidation of volatiles and char was observed at the stagnation point with single particles subjected to oxidizer streams with  $O_2 \geq 32\%$  (w/w) matches with the velocities at transition in the packed beds from the earlier studies. Simultaneous volatile-char oxidation and decrease in reaction zone thickness from a few particles to one particle diameter observed post-transition in packed beds support the theory.

**Keywords:** thermo-chemical conversion; ligno-cellulosic biomass; extinction strain rate; non-premixed ‘volatiles’ flame; packed bed; counter-current flame propagation;

## 1 Introduction

Counter-current packed bed is a commonly used configuration for laboratory studies (Varunkumar 2014; Jaganathan 2019), and small to medium scale (up to a 500 kWth) gasification systems (Barker 1996; Dasappa et al. 2004; Finland 2002; Wu et al. 2002). Schematic of a canonical configuration is shown in Fig. 1, in which the oxidizer flow direction is opposite to that of the flame propagation direction.

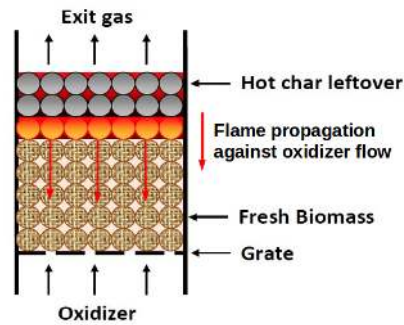


Figure 1: Counter current packed bed biomass gasification system.

Earlier study of Varunkumar, Rajan, and Mukunda (2013) with air as

oxidizer, was extended to mixtures of O<sub>2</sub>-N<sub>2</sub>/CO<sub>2</sub>/steam by Jaganathan and Varunkumar (2019); Jaganathan, Mohan, and Varunkumar (2019). Their results show that the fuel flux as a function of oxidizer mass flux exhibits universality - that is, the normalized fuel mass flux when plotted against volatiles equivalence ratio ( $\phi_v$ ) increases nearly linearly from fuel rich ( $\phi_v > 1$ ) conditions to near stoichiometry ( $\phi_v \sim 1$ ) and levels off beyond this. While this connection between volatiles stoichiometry and transition from gasification to combustion has been well established, the mechanism of transition is not well understood.

Studies on flame propagation with air as oxidizer in transparent reactors by Varunkumar, Rajan, and Mukunda (2013) have shown that the gasification-to-combustion regime transition is accompanied by *the blow-off of envelope diffusion flame* around individual particles to the char layer downstream. This leads to reduction in reaction zone thickness to one particle diameter from a few particle diameters and simultaneous volatiles-char oxidation (consistent with the visual observation of glowing char unlike in the gasification regime; refer Fig. 5.10 in Varunkumar 2014).

From Varunkumar, Rajan, and Mukunda (2013) it is known that the gasification-to-combustion regime transition occurs in the superficial velocity range ( $V_s$ ) of 15-18 cm/s. Accounting for bed porosity ( $\epsilon$ ) of 0.37 as mentioned in their study, the local velocity ( $V_s/\epsilon$ ) experienced by the particles is between 40 – 49 cm/s. This corresponds to an imposed strain rate ( $a_{packed-bed}$ ) of 203-244 s<sup>-1</sup>, estimated using Eq. 1, where  $R$  is the radius of the particle (4 mm).

$$a_{packed-bed} = \frac{2V_s}{\epsilon R} \quad (1)$$

Preliminary single particle experiments with air showed that the envelope

diffusion flame transitions to wake flame at around the same strain rate. This led us to hypothesize that the gasification-to-combustion regime transition is controlled by the extinction of the envelope ‘volatiles-flame’ (referred to as v-flame herein) around the particles in the de-volatilization zone.

But it is also well known that even under close to quiescent conditions, single particles burning in enriched air ( $O_2 > 50\%$  w/w) undergo simultaneous volatiles-char oxidation. This is due to the proximity of the gas phase flame to the surface compared to that with air, leading to oxygen access to char, especially under strained conditions. To test this, experiments were conducted with single biomass particles to determine the strain rate at transition from envelope flame to either wake flame (expected in the case of oxidizers with  $O_2 < 23\%$  w/w) or simultaneous volatiles-char oxidation (expected for  $O_2 > 23\%$  w/w).

## 2 Experimental methodology

Single particle experiments were performed to identify the flow conditions at which the envelope non-premixed v-flame transitions to either a wake flame or to simultaneous volatile-char combustion at the stagnation point, whichever occurred earlier. Corresponding strain rate was estimated from the measured oxidizer flow (using mass flow controllers) and the particle radius using Eq. 2.

$$a_{single-particle} = \frac{2V_\infty}{R} \quad (2)$$

The schematic of the experimental setup is shown in Fig. 2. The experimental setup consists of a cylindrical steel reactor of 100 mm diameter with a grate above a settling chamber. Flow uniformity is ensured by placing two

layers of steel balls of 2 mm diameter on the grate. Flow rates of gases were measured by mass flow controllers. Oxidizer component gases, namely, O<sub>2</sub> and N<sub>2</sub>/CO<sub>2</sub> were mixed in required proportions upstream of the reactor.

The composition of the oxidizer in the current work is reported on a mass basis (w/w). The particle was suspended in the oxidizer stream with the help of a pin. Oorja pellets of two different diameters (8 & 9 mm) and wood pellets of 9 mm are used in the current study. Table 1 summarizes the properties of the biomass used in the current work. Relevant properties of particles in the packed beds from references used for comparison in the current study are presented in Table 2.

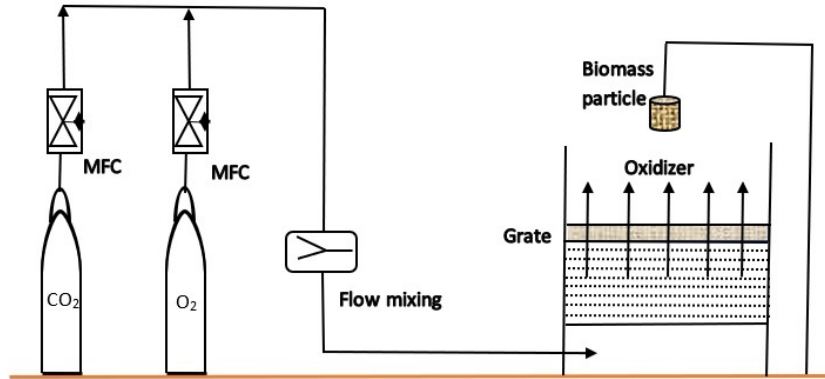


Figure 2: Schematic of the single particle setup.

Table 1: Properties of biomass used in the current study.

Properties	Oorja pellet	Wood pellet
Density (kg/m <sup>3</sup> )	1150	1260
Shape	cylindrical	cylindrical
Shape (d × l)	9 × 12 mm 8 × 7 mm	9 × 12 mm
Volatile content (DAF) %	83	84.7
Char content (DAF) %	17	15.3

Table 2: Properties of biomass used in the referenced studies.

Property	Oorja pellet (Varunkumar et al., 2013)	Oorja pellet (Jaganathan et al., 2019)	Wood pellet (Jaganathan et al., 2019)
Density (kg/m <sup>3</sup> )	1260	1150	1260
Shape	cylindrical	cylindrical	cylindrical
Dimensions in mm (d × l)	8 × 15-20	8 × 15-20	9 × 10-40
Bulk density (kg/m <sup>3</sup> )	794	630	664
Bed porosity	0.37	0.45	0.47

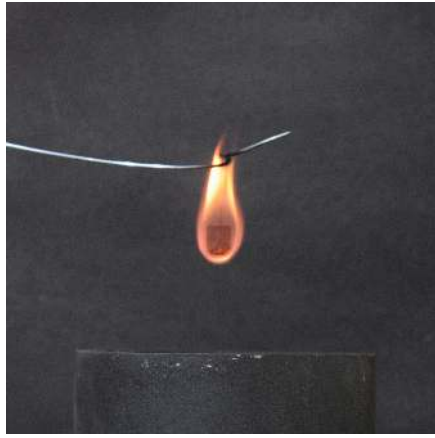
The suspended biomass particle was ignited using a lighter flame. A particle is considered ignited if a stable envelope diffusion flame surrounds it under quiescent conditions. During ignition, it was ensured that the entire particle is engulfed in the lighter flame so that the particle surface is not exposed to oxidizing conditions; this was done to avoid char ignition. After ignition, the reactor was moved underneath the particle and thereby exposing the particle to a steady uniform stream of oxidizer flow. Flame behavior was visually determined as one of the following three cases - (1) envelope v-flame (Fig. 3(a)), (2) wake flame (Fig. 3(b)) or (3) simultaneous volatiles-char oxidation (Fig. 3(c)).

In Fig. 3, the three possible states of the flame around a particle in a stream of oxidizer are shown. With air at free stream velocities < 29 cm/s, the flame envelopes the particle similar to that of a classical droplet burning case (see Fig. 3(a)). If the air velocity exceeds 38 cm/s, the volatiles are driven off from the stagnation point and are burnt in the wake region of the particle (see Fig. 3(b)). Further increasing the airflow rate would cause the volatiles to be driven off without oxidation with char combustion at the stagnation point.

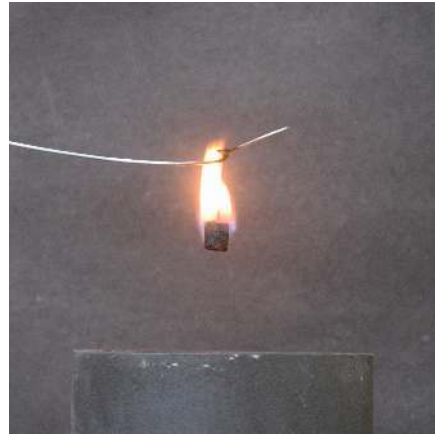
Simultaneous volatile-char combustion was identified by the glow of the char surface in addition to the presence of an envelope flame at the stagnation point. When a classical diffusion flame is formed at low strain rates, char surface appeared dark without any glow surrounded by the envelope flame. As the oxidizer mass flux is increased, the envelope diffusion flame is strained allowing for a leak of oxidizer to the char surface. This caused a discernible glow on the char surface at the stagnation point in addition to a stable v-flame encompassing the particle (refer Fig. 3(c)).

It is important to note that the change in diameter of the biomass particle during devolatilization is about 10% (Mukunda et al. 1985). Also, the volatile release rate is the same irrespective of particle density for a fixed ambient condition (Jaganathan, Kalyani, and Varunkumar 2017). Therefore, the time of exposure of the ignited particle to the oxidizer stream will not affect the transition strain rate as long as it is not too close to the point of complete devolatilization and the measured transition strain rate is universal (independent of particle density). To confirm that the extinction observed is due to the flow and not due to complete devolatilization at the stagnation point, the oxidizer source was removed and reintroduced to check for the presence of v-flame. A set of experiments with any given O<sub>2</sub> fraction were started with velocities that allowed the presence of a classical envelope v-flame. Then the oxidizer flow rate was gradually increased until the v-flame transitions to either a wake flame or simultaneous volatiles-char oxidation at the stagnation point.

The flow condition at transition of the envelope v-flame to the wake flame is quantified by the strain rate of the single particle ( $a_{single-particle}$ ) given by Eq. 2, where  $V_\infty$  is the free stream oxidizer velocity,  $R$  is the radius of the particle.



(a) v-flame around Oorja pellet at  $77 \text{ s}^{-1}$  with air



(b) wake flame around Oorja pellet at  $187 \text{ s}^{-1}$  with air



(c) volatiles-char oxidation around Oorja pellet at  $270 \text{ s}^{-1}$  with 60%  $\text{O}_2$  and 40%  $\text{CO}_2$ .

Figure 3: An example of v-flame, wake flame and simultaneous volatiles-char oxidation

### 3 Results and discussions

Experiments indicate that the transition is driven by extinction of v-flame for  $\text{O}_2 \leq 23\%$  (w/w). For  $\text{O}_2 \geq 32\%$  (w/w), the transition is driven by simultaneous oxidation of volatiles-char at the stagnation point. Therefore, these two cases are discussed in separate sections here.



### 3.1 Extinction of non-premixed v-flame

Flame type under different free-stream velocities with air as oxidizer is summarized in Table 3.

Table 3: Nature of the volatile flame around a single particle air is the oxidizer with Oorja pellets of  $8 \times 7$  mm as fuel.

$\dot{Q}$ (lpm)	$V_\infty$ (cm/s)	$a_{single-particle}$ ( $s^{-1}$ )	Flame type
10	2.5	12.5	classical flame
40	10	50	classical flame
70	17.4	87	classical flame
90	22.3	111.5	classical flame
120	29.9	149.5	classical flame
150	37.6	188	wake flame
200	49.7	248.5	wake flame
250	62	310	wake flame

The point of extinction occurs at a velocity of around 38 cm/s corresponding to an extinction strain rate of  $188 s^{-1}$ . As brought out earlier, conditions in packed-bed at transition point corresponds to a strain rate range of  $203 - 244 s^{-1}$ . A comparison of the strain rate experienced by the particles in the bed at the transition with that experienced by a single particle indicates that the transition is caused by the extinction of the v-flame. Combustion of volatiles in the wake and char at the stagnation point (Varunkumar, Rajan, and Mukunda 2013) also supports this hypothesis.

In Table 4, the extinction strain rate for wood pellets with air, and Oorja pellets of dimensions  $9 \text{ mm} \times 12 \text{ mm}$  with air, 19 and 23%  $O_2$  (rest  $CO_2$  on mass basis) cases and the corresponding gasification-to-char oxidation transition flow conditions in a packed bed (from Jaganathan and Varunkumar 2019) are summarized. With air as the oxidizer, single particles of wood pellets transition from v-flame to wake flame in the velocity range of 33–40 cm/s, while the range for Oorja pellets is 33–42.4 cm/s. This correspond to

an extinction strain rate range of 147–177 s<sup>-1</sup> and 147–188 s<sup>-1</sup> respectively for wood and Oorja pellets. For the case with 19% and 23% O<sub>2</sub> (rest CO<sub>2</sub>), the transition velocity ranges are 21–25 cm/s and 25–32 cm/s respectively. This corresponds to an extinction strain rate range of 93–111 s<sup>-1</sup> and 111–142 s<sup>-1</sup> with 19% and 23% O<sub>2</sub> fraction in the oxidizer respectively for the single particles of Oorja pellets. The transition in the bed for the corresponding oxidizer compositions lie in the same range as can be seen from Table 4 (computed using data taken from Jaganathan and Varunkumar 2019 and Eq. 1). This indicates that the mechanism that governs the transition in packed beds for low oxygen cases ( $\leq 23\%$  w/w) is the extinction of the non-premixed v-flame.

Table 4: Flow condition at the extinction of envelope v-flame around single particle and transition conditions in a bed. Particles are Oorja pellets unless mentioned otherwise; \* - wood pellet.

Oxidizer (w/w)	$a_{single-particle}$ (s <sup>-1</sup> )		$a_{packed-bed}$ (s <sup>-1</sup> )	
	Min	Max	Min	Max
Air	147	189	203	244 <sup>a</sup>
	147	189	167 <sup>b</sup>	-- <sup>b</sup>
	147*	177*	142 <sup>*b</sup>	212 <sup>*b</sup>
O <sub>2</sub> /CO <sub>2</sub> (19/81)	93	111	111 <sup>b</sup>	166.5 <sup>b</sup>
O <sub>2</sub> /CO <sub>2</sub> (23/77)	111	142	84 <sup>b</sup>	165 <sup>b</sup>

<sup>a</sup> - Varunkumar, Rajan, and Mukunda 2013

<sup>b</sup> - Jaganathan and Varunkumar 2019

### 3.2 Simultaneous oxidation of volatiles-char at the stagnation point

It was observed that with high O<sub>2</sub> fractions in the oxidizer streams (32, 37 and 42% on mass basis), as the oxidizer velocity is increased beyond a particular value, in addition to a gas phase flame, the char starts glowing at

the stagnation point. This is due to the combination of proximity of flame close to surface and high flame strain ( $> 177 \text{ s}^{-1}$ ), causing  $\text{O}_2$  leak to the char surface. This leads to char oxidation at the stagnation point with a surrounding v-flame. Table 5 presents the flow conditions at transition to simultaneous volatile-char combustion for 32, 37 and 42%  $\text{O}_2$  fraction in the oxidizer stream and the gasification-to-char oxidation transition observed in packed beds by Jaganathan and Varunkumar (2019). Since this is a transition and not extinction, the velocity at transition is reported instead of the strain rate.

Table 5: Flow condition at simultaneous volatile-char oxidation at stagnation point for a single particle and transition conditions in a bed from Jaganathan and Varunkumar (2019). Oorja pellets data is reported.

Oxidizer (w/w)	$v_t$ - single particle (cm/s)		$v_t$ - packed bed (cm/s)
	Min	Max	
$\text{O}_2/\text{CO}_2$ (32/68)	42	48	41.5
$\text{O}_2/\text{CO}_2$ (37/63)	42	51	-
$\text{O}_2/\text{CO}_2$ (42/58)	42	51	50

The transition from gasification to char oxidation in packed beds happens at a velocity that corresponds to simultaneous volatiles-char oxidation in single particles as can be seen from Table 5. Therefore, it can be concluded that the transition at higher  $\text{O}_2$  fractions is a result of simultaneous volatile-char oxidation at the stagnation point.

### 3.3 Gasification-to-combustion transition and its connection to volatile stoichiometry

From earlier studies (Varunkumar, Rajan, and Mukunda 2013; Jaganathan and Varunkumar 2019; Jaganathan, Mohan, and Varunkumar 2019) it can be seen that the ‘volatiles’ equivalence ratio ( $\phi_v$ ) ranges from 1.2-0.9 around

the transition to char combustion point in packed beds. This connection between transition and volatile stoichiometry is a convenient indicator for identifying optimal operating conditions for gasification - this is related to the fact that, post-transition, the char will not be available for reduction and hence not useful for gasification. But it is to be noted that the superficial velocity at transition provides the direct connection to transition. Notwithstanding these considerations, a summary of the conditions indicating connection between superficial velocity corresponding to volatiles stoichiometry and gasification-to-char combustion transition along with the single particle transition conditions are given in Table 6. Connection between volatiles stoichiometry and transition requires accounting for the effect of the differences between ignition and devolatilization times in controlling propagation and fuel consumption rate. We are currently working on developing a unified model towards establishing this connection.

Table 6: Mechanism of the gasification-to-char oxidation transition in a counter-current flame propagation in packed beds;  $V_s$  - superficial velocity at  $\phi_v \sim 1$ ;  $V_e$  - superficial velocity corresponding to extinction; E - extinction; S - transition to simultaneous volatiles-char oxidation.

$Y_{O_2}$ (w/w %)	Condition at transition	Transition criteria
19%	$V_e \sim V_s$	E
23%	$V_e \sim V_s$	E
Air	$V_e \sim V_s$	E
32%	$V_e > V_s$	S
37%	$V_e > V_s$	S
42%	$V_e > V_s$	S

## 4 Conclusions

In this study, a combination of single particle experiments and analysis of literature data for packed beds is used to bring out the mechanism of

gasification-to-char combustion transition in packed beds. The transition is shown to be controlled by either the extinction of the non-premixed v-flame or simultaneous volatile-char oxidation at the stagnation point, whichever is reached earlier. For low O<sub>2</sub> fractions ( $\leq 23\%$  w/w), the governing criterion is the extinction of the non-premixed v-flame. As the O<sub>2</sub> fraction is increased, the reaction rates increase and therefore, the velocity required for extinction also increases. However, high mass flux of oxygen leads to the gas phase flame being closer to the surface (compared to the cases with O<sub>2</sub>  $\leq 23\%$  w/w) and a leak of O<sub>2</sub> to the char surface initiating simultaneous volatile-char combustion at the stagnation point. Hence at high O<sub>2</sub> fractions  $\geq 32\%$  on mass basis, transition is controlled by simultaneous volatile-char oxidation at the stagnation point. Connection between the gasification-to-char combustion transition and volatiles stoichiometry is identified and the need for an unified modeling framework to establish the basis of these connections is brought out.

## References

1. Barker, S.N. 1996. Gasification and pyrolysis-routes to competitive electricity production from biomass in the UK. *Energy Conversion and Management* 37:861-66.
2. Dasappa, S., P. J. Paul, H. S. Mukunda, N. K. S. Rajan, G. Sridhar, and H. V. Sridhar. 2004. Biomass gasification technology—a route to meet energy needs. *Current Science* 87:908-16.
3. Finland, O. P. E. T. 2002. Review of Finnish biomass gasification technologies. Technical Research Centre of Finland, 10-13. Technical Research Centre of Finland.

4. Jaganathan, V.M., A. Mani Kalyani, and S. Varunkumar. 2017. Unified Ignition–Devolatilization model for fixed bed biomass Gasification/Combustion. *Energy Procedia* 120:643-48.
5. Jaganathan, V. M., O. Mohan, and S. Varunkumar. 2019. Intrinsic hydrogen yield from gasification of biomass with oxy-steam mixtures. *International Journal of Hydrogen Energy* 44:17781-91.
6. Jaganathan, V. M., and S. Varunkumar. 2019. Net carbon-di-oxide conversion and other novel features of packed bed biomass gasification with O<sub>2</sub>/CO<sub>2</sub> mixtures. *Fuel* 244:545-58.
7. Leung, Dennis YC, X. L. Yin, and C. Z. Wu. 2004. A review on the development and commercialization of biomass gasification technologies in China. *Renewable and Sustainable Energy Reviews* 8:565-80.
8. Mukunda, H. S., P. J. Paul, U. Srinivasa, and N. K. S. Rajan. 1985. Combustion of wooden spheres—experiments and model analysis. *Symposium (International) on Combustion* 20:1619-28.
9. Varunkumar, S., 2014. Packed bed gasification-combustion in biomass based domestic stoves and combustion systems. PhD diss., Indian Institute of Science.
10. Varunkumar, S., N. K. S. Rajan, and H. S. Mukunda. 2013. Universal flame propagation behavior in packed bed of biomass. *Combustion Science and Technology*. 185:1241-60. Wu, C. Z., Huang, H., S. P. Zheng, and X. L. Yin. 2002. An economic analysis of biomass gasification and power generation in China. *Bioresource technology*. 83:65-70.